

Electron mobility in dilute GaAs bismide and nitride alloys measured by time-resolved terahertz spectroscopy

D. G. Cooke^{a)} and F. A. Hegmann

Department of Physics, University of Alberta, Edmonton, Alberta T6G 2G7, Canada

E. C. Young

Department of Materials Engineering, University of British Columbia, Vancouver V6T 1Z4, Canada

T. Tiedje

*Department of Physics and Astronomy, University of British Columbia, Vancouver V6T 1Z4, Canada and
Department of Electrical and Computer Engineering, University of British Columbia, Vancouver
V6T 1Z4, Canada*

(Received 17 May 2006; accepted 18 July 2006; published online 18 September 2006)

We report time-resolved terahertz spectroscopy measurements of the electronic transport properties of dilute GaAs bismide and nitride alloys. The electron mobility for GaAs_{1-y}Bi_y ($y=0.84\%$) extracted from Drude fits to the transient complex conductivity was ~ 2800 cm²/V s at a carrier density of 2.7×10^{18} cm⁻³, close to the mobility of 3300 cm²/V s measured for GaAs at a similar carrier density. The electron mobility did not decrease significantly for Bi concentrations up to 1.4%. In contrast, the GaN_xAs_{1-x} ($x=0.84\%$) and GaN_xAs_{1-x-y}Bi_y ($x=0.85\%$, $y=1.4\%$) films exhibited non-Drude behavior with a highly reduced electron mobility and suppressed conductivity at low frequencies indicative of carrier localization. © 2006 American Institute of Physics.

[DOI: 10.1063/1.2349314]

The alloying of GaAs with small amounts of N or Bi produces an anomalously large reduction in the band gap, commonly referred to as giant band gap bowing.¹ The dilute nitride alloys, when combined with In, can be lattice matched to GaAs and are useful in long wavelength lasers,² solar cells,³ and heterojunction bipolar transistors.⁴ Although N and Bi are isoelectronic with As, the electronic structures of these atoms are sufficiently different from As that they behave more like impurities than conventional III-V alloying elements. In the case of the dilute nitride alloy, the band gap reduction is due to the resonant interaction of a nitrogen state with the bottom of the conduction band.⁵ Similarly, for the Bi alloy, the band gap reduction is believed to be due to a resonant interaction with the top of the valence band.⁶ The dilute nitride alloys show strong impurity scattering for electrons⁷ and carrier localization effects⁸ consistent with a strong interaction between N and the states at the bottom of the conduction band. This imposes severe limitations on device applications based on these nitride alloys. The effect of dilute Bi alloying on the transport properties of GaAs is, however, unknown. In this letter, we present experimental evidence that alloying GaAs with Bi does not significantly affect the electron mobility μ_e in contrast to the effect of N. Using dilute Bi alloying to lower the band gap energy without compromising the electron mobility should be important for device applications that currently use nitride alloying.

We use time-resolved terahertz spectroscopy (TRTS) to monitor the transient photoconductive (PC) decay of GaNAs, GaAsBi, and GaNAsBi samples after optical injection of carriers with 400 nm, 100 fs light pulses. The transient complex ac conductivity of GaAsBi is found to be well described by a simple Drude model, revealing an electron mobility that is relatively unaffected by dilute Bi doping compared to a bulk

GaAs reference. GaNAs and GaNAsBi, however, show signs of carrier localization in the suppression of the real part of the complex conductivity at low frequencies, consistent with localized states in the conduction band associated with N clustering.^{8,9}

In this study, three GaAs_{1-y}Bi_y films ($y=0.84\%$, 1% , and 1.4% , thicknesses of 260, 200, and 260 nm, respectively), one 225 nm thick GaN_xAs_{1-x} film ($x=0.84\%$), and one 170 nm thick GaN_xAs_{1-x-y}Bi_y ($x=0.85\%$, $y=1.4\%$) film were compared to a reference sample consisting of a 200 nm thick GaAs buffer layer. The films were grown by solid-source molecular-beam epitaxy on (001) GaAs substrates following growth of 200 nm thick GaAs buffer layers at 580 °C. Activated N was provided by a low-pressure rf plasma source. Conventional effusion cells were used for Ga, Al, and Bi, and the As₂ source was a two zone cracker cell. The GaNAs film was grown at a substrate temperature of 440 °C, while the bismides were grown at lower temperatures (GaAsBi at 340–370 °C, GaNAsBi at 380 °C) and reduced Ga/As flux ratios (~ 1) in order to achieve Bi incorporation. The reference GaAs layer was grown at 550 °C. Film compositions were determined by simulation of high-resolution x-ray diffraction measurements.¹⁰

TRTS is an optical-pump far-infrared-probe technique used to monitor the photoinduced conductivity of materials with subpicosecond time resolution.^{11–15} In these experiments, the 800 nm, ~ 100 fs output from a kilohertz multipass amplified laser system is frequency doubled in a beta barium borate crystal to a 400 nm pump pulse. A smaller portion of the fundamental is used to generate an ~ 0.5 ps, terahertz probe pulse with Fourier components from 0.3 to 3 THz by optical rectification in a 0.5 mm thick [110]-oriented ZnTe crystal. The sample is mounted on a 1.5 mm aperture, at the focus of the terahertz probe beam. All measurements were taken at room temperature. The pump pulse excites electrons and holes in the sample at normal incidence

^{a)}Electronic mail: dcooke@phys.ualberta.ca

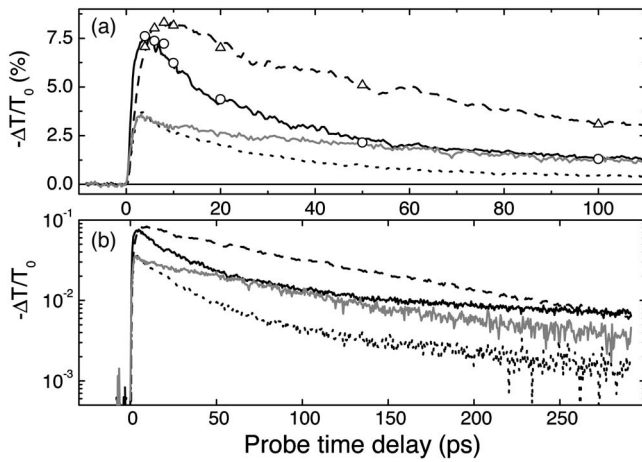


FIG. 1. (a) Linear and (b) semilog plots of the negative differential terahertz transmission ($-\Delta T/T_0$) for the GaAs buffer layer (solid black), GaAsBi (0.84% Bi) (dashed), GaNAs (0.84% N) (dotted), and GaNAsBi (0.85% N, 1.4% Bi) (gray) samples, at a pump fluence of $3.7 \mu\text{J}/\text{cm}^2$. The open symbols in (a) are carrier densities normalized to the peak $-\Delta T/T_0$, derived from the Drude fits to the complex conductivity for the GaAs buffer (\circ), and GaAsBi (Δ) samples.

with a fluence of $3.7 \mu\text{J}/\text{cm}^2$. The terahertz pulse then probes the transient photoconductivity in the sample at some time delay (Δt) after the initial excitation by the pump pulse. A third portion of the 800 nm fundamental is used for coherent free-space electro-optic detection of the transmitted terahertz electric field in another 0.5 mm thick ZnTe crystal, so that the amplitude and phase of the electric field are measured. This permits extraction of both the real and imaginary parts of the complex conductivity $\tilde{\sigma}(\omega) = \sigma_1(\omega) + i\sigma_2(\omega)$ without the use of Kramers-Kronig analysis.¹¹ By varying the time delay (Δt) between the pump and terahertz probe, the photoinduced conductivity of the sample can be mapped with subpicosecond resolution. The complex transmission function, obtained by taking the ratio of the Fourier transforms of the terahertz wave forms with (pump) and without (ref) photoexcitation, is related analytically to the conductivity of the excited layer by^{13–15}

$$\tilde{T}(\omega) = \frac{\tilde{E}_{\text{pump}}(\omega)}{\tilde{E}_{\text{ref}}(\omega)} = \frac{N + 1}{N + 1 + Z_0 d \tilde{\sigma}(\omega)}, \quad (1)$$

where N is the index of refraction of the substrate at terahertz frequencies (taken as 3.6 for bulk GaAs) and $Z_0 = 377 \Omega$. The thickness of the conducting layer, d , is approximately the pump penetration depth of 15 nm in bulk GaAs.¹³ In this study it is assumed that the electrons dominate the transient PC response, since for GaAs the electron mobility μ_e is approximately ten times that of the hole mobility μ_h .

While measuring the entire terahertz wave form for each probe time delay affords frequency-resolved spectroscopy, the lengthy data acquisition times put a limit on the time resolution with which one can map out the PC decay. To resolve this, the peak terahertz electric field amplitude is monitored while scanning the pump-probe time delay. This is a measure of the terahertz attenuation averaged over the bandwidth of the pulse, where the negative differential terahertz transmission, $-\Delta T/T_0 = (T_{\text{ref}} - T_{\text{pump}})/T_{\text{ref}}$, is directly proportional to the PC of the sample for small $|\Delta T/T_0|$.^{13–15}

Figure 1 shows the $-\Delta T/T_0$ transients for the GaAsBi (0.84% Bi), GaNAs (0.84% N), GaNAsBi (0.85% N, 1.4% Bi) samples, and the reference GaAs buffer layer.

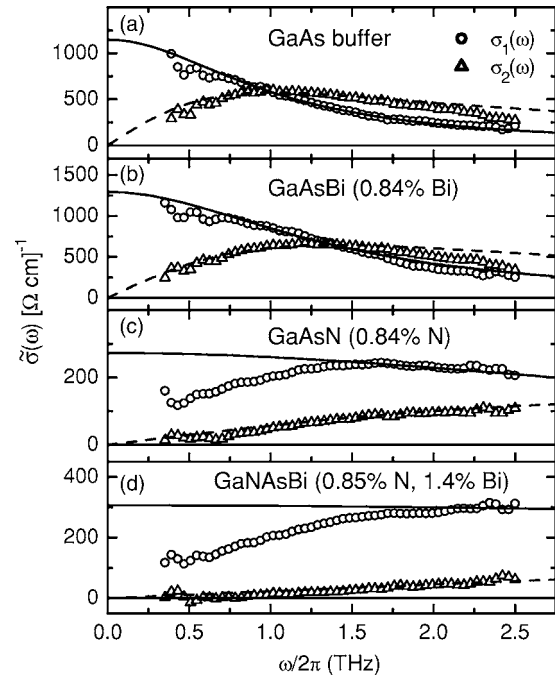


FIG. 2. Extracted complex conductivity for (a) GaAs buffer layer, (b) GaAsBi (0.84% Bi) (c) GaNAs (0.84% N), and (d) GaNAsBi (0.85% N, 1.4% Bi) 10 ps after 400 nm excitation at a fluence of $3.7 \mu\text{J}/\text{cm}^2$. The solid and dashed lines are fits to the real and imaginary parts of the Drude conductivity with (a) $\omega_p/2\pi = 46 \pm 1$ THz, $\tau = 157 \pm 7$ fs, (b) $\omega_p/2\pi = 57 \pm 1$ THz, $\tau = 115 \pm 4$ fs, (c) $\omega_p/2\pi = 48 \pm 2$ THz, $\tau = 35 \pm 3$ fs, and (d) $\omega_p/2\pi = 86 \pm 2$ THz, $\tau = 12 \pm 1$ fs.

Bi), and the reference GaAs buffer layer. The peak $-\Delta T/T_0$ is proportional to the electron mobility given the same excitation density. The significantly lower GaNAs and GaNAsBi signals compared to the buffer and bismide samples are a strong initial indication that N severely reduces carrier mobility while Bi does not. The PC decay for the GaAs (GaNAs) samples is well described by a biexponential decay with fast and slow time constants of 22 (23) and 260 (170) ps, respectively. This fast decay is likely due to surface recombination, which is efficient since the majority of carriers are injected within 20 nm of the surface. The GaAsBi film, however, showed a clear single exponential decay of 101 ± 1 ps, as seen in Fig. 1(b). This indicates a single, fast free-carrier depletion mechanism which is not likely due to surface recombination, since this would lead to a different nonexponential decay.¹² A more likely explanation is due to a distribution of trap centers distributed throughout the film. The GaNAsBi film showed an approximately exponential decay with a time constant of 86 ps.

Figure 2 presents the frequency-resolved complex conductivity for the samples shown in Fig. 1, 10 ps after photoexcitation. At 400 nm excitation, photoexcited carriers have sufficient energy to scatter into satellite valleys in GaAs. Within ~ 6 ps, carriers have relaxed to the higher mobility Γ valley and an accurate, low-field mobility value can be obtained.¹² For the GaAs buffer layer, both $\sigma_1(\omega)$ and $\sigma_2(\omega)$ are well described by a simple Drude model, as shown in Fig. 2(a). Using a bulk GaAs electron effective mass, $m_{\text{GaAs}}^* = 0.067 m_e$, the simultaneous fitting of σ_1 and σ_2 to these data gives a carrier density $n = 1.8 \times 10^{18} \text{ cm}^{-3}$ and mobility $\mu_e = 4100 \text{ cm}^2/\text{V s}$, in good agreement with the maximum density of $2.6 \times 10^{18} \text{ cm}^{-3}$ calculated from the pump fluence and literature μ_e values.¹⁶

Examining the extracted conductivity data for the GaAsBi sample in Fig. 2(b), we see again that the complex conductivity is well described by a free-carrier Drude model with $\mu_e=3020 \text{ cm}^2/\text{V s}$ at $n=2.7 \times 10^{18} \text{ cm}^{-3}$ assuming $m^*=m_{\text{GaAs}}^*$. At a comparable carrier density of $2.2 \times 10^{18} \text{ cm}^{-3}$, the GaAs buffer layer showed $\mu_e=3300 \text{ cm}^2/\text{V s}$, only slightly higher than that of the bismide. This shows that the electron mobility in GaAsBi films is relatively insensitive to dilute Bi alloying. The higher concentration Bi (1.4%) sample showed the same electron mobility as the 0.84% sample at early times, indicating that the mobility is not significantly altered by increasing the Bi concentration up to 1.4%.

As seen in Fig. 2(c), the GaNAs conductivity shows a strong suppression in σ_1 at low frequencies that smoothly returns to Drude behavior above 1.56 THz. Such a reduction is consistent with the picture of localized cluster states within the conduction band, where long range transport (low frequency) is hindered by the cluster potential but transport over short distances (high frequency) is bandlike. From the high frequency Drude fits assuming $m^*=m_{\text{GaAs}}^*$, the mobility is $920 \text{ cm}^2/\text{V s}$ at $n=1.9 \times 10^{18} \text{ cm}^{-3}$, which is in good agreement with the intrinsic limitation on the electron mobility imposed by alloy scattering in $\text{GaN}_x\text{As}_{1-x}$ for $x \cong 0.01$ and $m^*=m_{\text{GaAs}}^*$.¹⁷

It has been proposed that the incorporation of Bi might improve the electronic properties of GaNAs by strain compensating the small N atom with the larger Bi atom.^{18,19} The appropriate concentration ratio of Bi to N to achieve lattice matching with GaAs has been reported to be 1.7.^{18,20} Figure 2(d) shows the conductivity results for the $\text{GaN}_x\text{As}_{1-x-y}\text{Bi}_y$ sample with $y \cong 1.7x$. Like the GaNAs sample, $\sigma_1(\omega)$ is highly suppressed at lower frequencies and merges with Drude behavior at higher ω . Drude fits to the high ω portion of the spectra, assuming $m^*=m_{\text{GaAs}}^*$, give a mobility of $320 \text{ cm}^2/\text{V s}$, reduced from the GaNAs mobility and indicating that the electronic properties are not improved by codoping with Bi. We note that our measurements show that a dc measurement ($\omega=0$) of the mobility will be smaller than these high frequency estimates.

A possible complication in these measurements is the diffusion of carriers into the underlying high μ buffer layer. GaAsBi may have little conduction band offset with GaAs, whereas GaNAs has a significant offset which acts as a barrier to diffusion of electrons. To ensure that the high μ observed in the GaAsBi was not due to electron transfer to the buffer layer, a similar film was grown on a $1.4 \mu\text{m}$ $\text{Al}_{0.27}\text{Ga}_{0.63}\text{As}$ barrier layer to confine carriers to the GaAsBi film. In addition to confining the electrons, the $\text{Al}_{0.27}\text{Ga}_{0.63}\text{As}$ barrier layer also has a low mobility. Without the AlGaAs barrier, the extracted GaAsBi μ_e values are constant at $\sim 2800 \text{ cm}^2/\text{V s}$ for $\Delta t=4-10$ ps and then slowly rise due to diffusion into the buffer region. With the AlGaAs barrier, μ_e is constant at $2800 \text{ cm}^2/\text{V s}$ for $\Delta t \leq 50$ ps, reflecting the 300 meV conduction band offset limiting diffusion into the buffer layer. We therefore conclude that diffusion does not influence the extracted mobility values in the nonbarrier samples for $\Delta t < 10$ ps. Table I summarizes these early time ($\Delta t \leq 10$ ps) mobility results for all samples investigated.

In conclusion, we have used TRTS to characterize the carrier transport mechanisms in dilute GaAs nitride and bis-

TABLE I. Extracted electron mobilities from Drude fits to the complex conductivity in various samples for early delay times $\Delta t=4-10$ ps, with a 400 nm pump fluence of $3.7 \mu\text{J}/\text{cm}^2$ ($n \sim (2-3) \times 10^{18} \text{ cm}^{-3}$).

Sample	μ_e ($\text{cm}^2/\text{V s}$)
GaAs buffer layer	3300 ± 100
$\text{GaAs}_{1-y}\text{Bi}_y$ ($y=0.84\%$)	2800 ± 100
$\text{GaAs}_{1-y}\text{Bi}_y$ ($y=1.0\%$, AlGaAs barrier)	2800 ± 100
$\text{GaAs}_{1-y}\text{Bi}_y$ ($y=1.4\%$)	2700 ± 100
$\text{GaN}_x\text{As}_{1-x}$ ($x=0.84\%$)	920 ± 80^a
$\text{GaN}_x\text{As}_{1-x-y}\text{Bi}_y$ ($x=0.85\%$, $y=1.4\%$)	340 ± 30^a

^aDerived from high frequency fits to the Drude model.

mide alloys. We find that the electron mobility is significantly reduced in GaNAs, with non-Drude behavior at low frequencies due to the presence of localized states. In GaAsBi, however, we find Drude behavior with $\mu_e=2800 \text{ cm}^2/\text{V s}$ at $n=2.7 \times 10^{18} \text{ cm}^{-3}$, which is almost unchanged relative to GaAs with $\mu_e=3300 \text{ cm}^2/\text{V s}$ at $n=2.2 \times 10^{18} \text{ cm}^{-3}$. We find no further reduction in μ_e for Bi concentrations up to 1.4%, showing that the band gap of GaAs can be reduced without significantly degrading the electron transport properties by dilute Bi alloying. Finally, the electronic properties of the quaternary alloy GaNAsBi were found to be further degraded over GaNAs by incorporation of Bi, again showing strong deviation from Drude conductivity with low frequency $\sigma_1(\omega)$ suppression.

The authors acknowledge financial support from NSERC, CIPI, and iCORE.

¹W. G. Bi and C. W. Tu, Appl. Phys. Lett. **70**, 1608 (1997).

²N. Laurand, S. Calvez, H. D. Sun, M. D. Dawson, J. A. Gupta, and G. C. Aers, Electron. Lett. **42**, 29 (2006).

³A. J. Ptak, D. J. Friedman, S. Kurtz, and R. C. Reedy, J. Appl. Phys. **98**, 094501 (2005).

⁴P. M. Asbeck, R. J. Welty, C. W. Tu, H. P. Xin, and R. E. Welsler, Semicond. Sci. Technol. **17**, 898 (2002).

⁵L. Bellaiche, S.-H. Wei, and Alex Zunger, Phys. Rev. B **54**, 17568 (1996).

⁶Y. Zhang, A. Mascarenhas, H. P. Xin, and C. W. Tu, Phys. Rev. B **63**, 161303 (2001).

⁷R. Mouillet, L. A. de Vaulchier, E. Deleporte, Y. Guldner, L. Travers, and J. C. Harmand, Solid State Commun. **126**, 333 (2003).

⁸P. R. C. Kent and A. Zunger, Phys. Rev. Lett. **86**, 2613 (2001).

⁹F. Ishikawa, G. Mussler, K.-J. Friedland, H. Kostial, K. Hagenstein, L. Däweritz, and K. H. Ploog, Appl. Phys. Lett. **87**, 262112 (2005).

¹⁰S. Tixier, M. Adameyk, T. Tiedje, S. Francoeur, A. Mascarenhas, P. Wei, and F. Schiettekatte, Appl. Phys. Lett. **82**, 2245 (2003).

¹¹C. A. Schmuttenmaer, Chem. Rev. (Washington, D.C.) **104**, 1759 (2004).

¹²M. C. Beard, G. M. Turner, and C. A. Schmuttenmaer, Phys. Rev. B **62**, 15764 (2000).

¹³D. G. Cooke, F. A. Hegmann, Y. I. Mazur, W. Q. Ma, X. Wang, Z. M. Wang, G. J. Salamo, M. Xiao, T. D. Mishima, and M. B. Johnson, Appl. Phys. Lett. **85**, 3839 (2004).

¹⁴D. G. Cooke, A. N. MacDonald, A. Hryciw, A. Meldrum, J. Wang, Q. Li, and F. A. Hegmann, Phys. Rev. B **73**, 193311 (2006).

¹⁵R. P. Prasankumar, A. Scopatz, D. J. Hilton, A. J. Taylor, R. D. Averitt, J. M. Zide, and A. C. Gossard, Appl. Phys. Lett. **86**, 201107 (2005).

¹⁶W. Walukiewicz, L. Lagowski, L. Jastrzebski, M. Lichtensteiger, and H. C. Gatos, J. Appl. Phys. **50**, 899 (1979).

¹⁷S. Fahy and E. P. O'Reilly, Appl. Phys. Lett. **83**, 3731 (2003).

¹⁸A. Janotti, S. H. Wei, and S. B. Zhang, Phys. Rev. B **65**, 115203 (2002).

¹⁹A. Mascarenhas, Y. Zhang, J. Verley, and M. J. Seong, Superlattices Microstruct. **29**, 395 (2001).

²⁰S. Tixier, S. E. Webster, E. C. Young, T. Tiedje, S. Francoeur, A. Mascarenhas, P. Wei, and F. Schiettekatte, Appl. Phys. Lett. **86**, 112113 (2005).